



1 **Vegetation-mediated surface soil organic carbon formation and potential carbon**
2 **loss risks in Dongting Lake floodplain, China**

3 Liyan Wang^{1, 2, 3}, Zhengmiao Deng^{1, 2}, Yonghong Xie^{1, 2}, Tao Wang^{1, 2}, Feng Li^{1, 2}, Ye'ai Zou^{1, 2},

4 Buqing Wang⁴, Zhitao Huo⁴, Cicheng Zhang⁵, Changhui Peng⁶, Andrew Macrae⁷

5 ¹ *Institute of Subtropical Agriculture, Chinese Academy of Sciences, Changsha 410125, China*

6 ² *Dongting Lake Station for Wetland Ecosystem Research, Institute of Subtropical Agriculture,*

7 *Chinese Academy of Sciences, Changsha 410125, China*

8 ³ *University of Chinese Academy of Sciences, Beijing 100049, China*

9 ⁴ *Changsha General Survey of Natural Resources Center, China Geological Survey, Changsha*
10 *410600, China*

11 ⁵ *College of Geographic Science, Hunan Normal University, Changsha 410081, China*

12 ⁶ *Department of Biological Sciences, the University of Québec at Montreal, Montreal, QC H3C 3P8,*
13 *Canada*

14 ⁷ *Centro de Ciências da Saúde (CCS), Universidade Federal do Rio de Janeiro, BR 21941902, Brazil*

15
16 **Corresponding author:** Zhengmiao Deng (dengzhengmiao@163.com) and
17 Yonghong Xie (yonghongxie@163.com)
18

19 **Abstract**

20 Sources and stabilization mechanisms of soil organic carbon (SOC) fundamentally
21 govern the carbon sequestration potential of wetland ecosystems. Nevertheless,
22 systematic investigations regarding SOC sources and molecular stability remain scarce
23 in floodplain wetland environments. This study employed dual analytical approaches
24 (stable isotope analysis and ¹³C nuclear magnetic resonance spectroscopy) to
25 characterize surface SOC composition across three dominant vegetation communities
26 (*Miscanthus*, *Carex*, and mudflat) in Dongting Lake floodplain wetlands. Key findings
27 revealed: (1) Significantly elevated SOC concentrations in vegetated communities
28 (*Miscanthus*: 13.76 g kg⁻¹; *Carex*: 12.98 g kg⁻¹) compared to unvegetated mudflat (6.88
29 g/kg); (2) Distinct δ¹³C signatures across communities, with the highest isotopic values
30 in *Miscanthus* (-22.67 ‰), intermediate in mudflat (-26.01 ‰), and most depleted
31 values in *Carex* (-28.25 ‰); (3) Bayesian mixing models identified autochthonous plant



32 biomass as the primary SOC source (*Miscanthus*: 53.3 ± 10.6 %, *Carex*: 52.4 % ± 11.6 %,
33 Mudflat: 47.5 ± 12.5 %); (4) Spatial heterogeneity in POM contributions across sub-
34 lakes, showing descending contributions from South (highest) > West > East (lowest)
35 Dongting Lake; (5) Molecular characterization revealed O-alkyl C dominance (27.3-
36 46.8 %), followed by alkyl C and aromatic C. Notably, *Miscanthus* soils exhibited
37 enhanced O-alkyl C content (Alip/Arom) and reduced aromaticity/hydrophobicity
38 indices, suggesting comparatively lower biochemical stability of its SOC pool. These
39 results highlight the critical role of vegetation-mediated SOC formation processes and
40 warn against potential carbon loss risks in *Miscanthus*-dominated floodplain
41 ecosystems, providing a scientific basis for carbon management of wetland soils.

42 **Keywords:** Floodplain wetland; Stable isotope; Soil carbon source; ^{13}C NMR; Organic
43 carbon stability

44 **1 Introduction**

45 Although wetlands occupy merely 5-8 % of the global terrestrial surface, they
46 disproportionately store 20-30 % of the terrestrial carbon, positioning them as pivotal
47 regulators in global carbon cycling (Kayranli et al., 2010; Köchy et al., 2015; Mitsch et
48 al., 2013). Small changes in wetland soil organic carbon (SOC) stocks may have large
49 feedback effects on climate-carbon cycle interactions. The long-term carbon
50 sequestration capacity of wetland ecosystems is jointly governed by two critical factors:
51 carbon input dynamics and biochemical stabilization mechanisms. Therefore, clarifying
52 the sources and stabilization pathways of wetland SOC is essential for optimizing
53 carbon sink management and enhancing climate change mitigation strategies.

54 In floodplain systems, the organic carbon in sediment derives from both
55 autochthonous (in-situ plant biomass and aquatic plankton) and allochthonous sources
56 (river-transported particulate organic matter, POM) (Robertson et al., 1999). Notably,
57 the relative contributions of these sources vary significantly across vegetation
58 communities, driven primarily by vegetation characteristics (e.g., biomass production
59 and litter composition) and hydrological regimes (e.g., flood duration, frequency, and
60 intensity). For example, in mangrove ecosystems, mangrove community SOC is mainly



61 derived from mangrove plant tissues, whereas adjacent *S. alterniflora* and tidal flats
62 exhibit stronger reliance on fluvially imported POM (Wang et al., 2024a). These source
63 differences across vegetation communities are further modulated by geomorphic
64 features (e.g., elevation, channel morphology) and anthropogenic disturbances (e.g.,
65 land-use changes). For example, topographic complexity determines the lateral
66 transport and deposition of POM in rivers, resulting in localized heterogenic carbon
67 accumulation. Despite these insights, critical knowledge gaps persist regarding
68 interspecific differences in carbon sourcing among co-occurring vegetation
69 communities within floodplain wetlands and the spatial scaling of these heterogeneities.
70 Stable carbon and nitrogen isotopes have been widely used to analyze the sources of
71 wetland SOC (Sasmito et al., 2020; Wu et al., 2021a).

72 SOC stability is defined as the capacity of organic compounds to
73 resist changes and/or losses (Doetterl et al., 2016). Enhanced SOC stability typically
74 corresponds with preferential accumulation of recalcitrant compounds that withstand
75 microbial degradation. ¹³C nuclear magnetic resonance (NMR) is widely used to
76 analyze the chemical composition of SOC, and can calculate the relative abundance of
77 various C functional groups closely related to SOC decomposition (Shen et al., 2018).
78 Biochemically recalcitrant components include alkyl-C and aromatic-C, whereas labile
79 components comprise O-alkyl-C and carbonyl-C (Skjemstad et al., 1994) .
80 Consequently, soils enriched in labile SOC fractions demonstrate heightened
81 vulnerability to carbon loss through accelerated decomposition pathways, particularly
82 under environmental disturbance. These molecular signatures are regulated by factors,
83 including vegetation inputs (via lignin/cellulose ratios and aliphatic content), soil
84 properties (clay-silt particle associations), and climatic controls on vegetation litter
85 decomposition (Cano et al., 2002; Chen et al., 2018; Liu et al., 2022; Preston et al.,
86 1994; Quideau et al., 2001; Wu et al., 2020). In floodplain environments, hydrologic
87 conditions further regulate SOC components by affecting oxygen supply and altering
88 microbial metabolism and enzyme activity (Kirk and Farrell, 1987; Boye et al., 2017).
89 However, there are insufficient studies on the sources and stability of SOC in floodplain



90 wetlands.

91 Dongting Lake, a Yangtze River-connected floodplain wetland, presents an ideal
92 natural laboratory for investigating these processes. Its elevation-dependent vegetation
93 zonation and complex topography create pronounced gradients in carbon source inputs
94 and stabilization conditions. Among soil carbon pools, surface SOC is more susceptible
95 to the effects of climate, hydrological conditions and human activities, resulting in a
96 high carbon turnover rate and requiring more attention. In this study, stable isotope
97 techniques were used to analyze the source of surface SOC and the stability of SOC
98 was further evaluated using the ^{13}C NMR method. The hypotheses of this study were
99 (1) with regard to vegetation communities, based on plant biomass, SOC content should
100 be the highest in the *Miscanthus* community, followed by the *Carex* community, with
101 the Mudflat exhibiting the lowest SOC content. From a spatial perspective, considering
102 the influence of topographic and hydrological characteristics, the SOC levels were
103 expected to follow a gradient, being highest in East Dongting Lake, intermediate in
104 South Dongting Lake, and lowest in West Dongting Lake. (2) SOC in *Miscanthus* and
105 *Carex* community would primarily originate from autochthonous plant sources due to
106 their high biomass production; in contrast, the source of SOC in the Mudflat would
107 primarily originate from allochthonous POM, and (3) due to the difference in sources,
108 the SOC structure in *Miscanthus* and *Carex* should be dominated by O-alkyl C, and the
109 SOC structure of the Mudflat should be dominated by aromatic C.

110

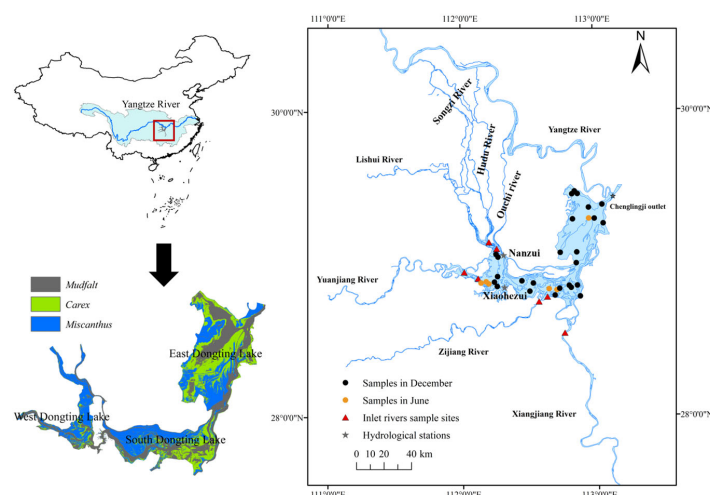
111 **2 Materials and methods**

112 **2.1 Study areas**

113 Dongting Lake (28°30'–30°20'N, 111°40'–113°10'E) is the second largest inland
114 freshwater lake in China, with an area of 2564 km². It comprises East Dongting Lake
115 (EDL, 1327.8 km²), West Dongting lake (WDL, 443.9 km²) and South Dongting Lake
116 (SDL, 920 km²) (Jun-Feng et al., 2001). The Lake is a typical river-connected lake that
117 mainly receives inflow from the Yangtze River through three channels (the Songzi,
118 Hudu, and Ouchi Rivers) and other four tributaries (the Xiang, Zi, Yuan, and Li Rivers)



119 and then outflows into the Yangtze River from the Chenglingji outlet (Deng et al., 2018).
 120 The lake's water level exhibits significant seasonal fluctuations, with flood periods
 121 occurring from June to October. From the water's edge to the uplands, the dominant
 122 vegetation communities include Mudflat communities, *Carex spp.* (Cyperaceae)
 123 communities, and *Miscanthus sacchariflorus* (Poaceae) communities (Xie et al.,
 124 2015). The study area is characterized by a humid subtropical monsoon climate with a
 125 mean annual temperature of 16.8°C and a mean annual precipitation of 1382 mm.



126
 127 **Figure 1.** Map of the study area and sampling sites (base map from ESRI).

128 2.2 Field sampling and parameter measurement

129 Soil sampling was conducted across three dominant vegetation during December
 130 2022, with supplementary Mudflat sediment sampling in June to account for
 131 hydrological accessibility constraints. The final sampling comprised 31 sampling sites
 132 (11 Mudflat, 8 *Carex* community, 12 *Miscanthus* community) with latitude and
 133 longitude recorded using a hand-held global positioning system (GPS). Notably, *Carex*
 134 communities in West Dongting Lake were excluded from sampling due to insufficient
 135 population density. At each sampling site, a 1x1 m sample plot was set up, and surface
 136 (0-20 cm, 500 g fresh soil) soil samples were collected from five points in the plot and
 137 mixed for subsequent analysis. For vegetated sites (*Carex* and *Miscanthus*
 138 communities), aboveground tissue, surface litter layer and belowground roots were



139 collected from the sample plots. All samples were transported to the laboratory. Soil
140 samples were air-dried in a cool, ventilated area, ground and passed through a 0.147
141 mm sieve for subsequent analysis. Plant material was dried at 60° C to a constant mass
142 and the dry weight was recorded prior to pulverization. Both SOC and plant organic
143 carbon content was quantified using the potassium dichromate-sulfuric acid oxidation
144 technique. The TN content of soil was measured using an elemental analyzer (Vario
145 MAX CNS, Elementar, Germany). The formula for calculating vegetation organic
146 carbon stocks (VOCS) is as follows:

$$147 \quad VOCS = A \times VB \times VOC \quad (1)$$

148 Where A is the vegetation distribution area (km²), VB is the vegetation biomass
149 (t/km²), VOC is the vegetation organic carbon content (g kg⁻¹).

150 **2.3 Inundation duration and runoff volume**

151 We used the hydrological data from Chenglingji, Xiaohezui, and Nanzui
152 hydrological stations to calculate the inundation time and runoff volume of EDL, SDL,
153 and WDL, respectively. The hydrological data from Chenglingji, Xiaohezui and Nanzui
154 have been widely used to analyze the hydrological characteristics of EDL, SDL and
155 WDL. Vegetation is classified as submerged when water levels exceed specific
156 elevations. Using daily water levels and elevation data from the Dongting Lake Wetland
157 DEM (Geospatial Data Cloud: <http://www.gscloud.cn>), we calculated vegetation-
158 specific inundation durations. The formula for calculating the inundation duration is as
159 follows:

160 The inundation duration (ID) was calculated as follows:

$$161 \quad ID = \sum_{WD>0}^n I_{WD} \quad (2)$$

$$162 \quad WD = WL - E \quad (3)$$

163 where WL is the water level at the Chenglingji (EDL), Xiaohezui (SDL), and Nanzui
164 (WDL) Hydrological Station, E is the elevation, I_{WD} is the number of days when $WD>0$,
165 and n is the number of days per year.

166 **2.4 Stable isotope analysis and mixing model**

167 The soil samples (2 g) were added to 0.5 mol/L hydrochloric acid reflections for



168 24 h to removal carbonates, then washed to neutrality with distilled water and dried at
169 55 °C. The treated soil samples were ground through a 0.147 mm sieve and used for
170 stable isotope measurements. $\delta^{13}\text{C}$ and $\delta^{15}\text{N}$ stable isotope ratios were measured using
171 a gas chromatography-isotope ratio mass spectrometer (Delta V advantage, Thermo
172 Fisher) and were calculated from the following equation:

$$173 \quad \delta(\text{‰}) = ((R_{\text{sample}}/R_{\text{standard}}) - 1) \times 1000 \quad (4)$$

174 where R_{sample} is the stable $^{13}\text{C}/^{12}\text{C}$ or $^{15}\text{N}/^{14}\text{N}$ isotope ratio of the sample, and R_{standard} is
175 stable the $^{13}\text{C}/^{12}\text{C}$ or $^{15}\text{N}/^{14}\text{N}$ isotope ratios of the international isotope standard (Vienna
176 Pee Dee Belemnite and N_2 in the atmosphere, respectively).

177 SOC potential sources include *Miscanthus* plant, *Carex* plant and Plankton, and
178 rivers suspended particulate organic matter (POM). In addition to plankton, we
179 collected other potential end-members for stable isotope analysis. Five samples of
180 aboveground tissues, surface litter and root of *Miscanthus* and *Carex* plants were
181 randomly sampled. Due to the construction of the Three Gorges Dam, the POM entering
182 Dongting Lake changed from three channels (the Songzi, Hudu, and Ouchi Rivers) to
183 four tributaries (the Xiang, Zi, Yuan, and Li Rivers) (Wang et al., 2024b). Therefore,
184 we collected POM at the inlets of the Xiang, Zi, Yuan, and Li Rivers into the lake. The
185 POM from the Yuan and Li Rivers served as the allochthonous end-members for WDL,
186 while the POM from the Xiang, Zi, Yuan, and Li Rivers served as the allochthonous
187 end-members for EDL and SDL (Fig. 1).

188 Source contributions were quantified using a Bayesian mixing model based on
189 $\delta^{13}\text{C}$ and $\delta^{15}\text{N}$. The MixSIAR model combines the advantages of SIAR and MixSIR. It
190 not only introduces fixed and random effects, but also incorporates source uncertainty.
191 These features endow the MixSIAR model with higher source analysis accuracy, and it
192 has been widely used in wetland sediments (Zhang et al., 2024).

193 **2.5 ^{13}C NMR analysis and spectral indices**

194 The chemical structure of SOC was determined by solid-state ^{13}C NMR
195 spectroscopy. In order to improve the signal-to-noise ratio, soil samples are pretreated
196 with hydrofluoric acid (HF) before ^{13}C NMR spectroscopy analysis. Soil samples (8.0



g) were placed into 100 mL plastic centrifuge tubes containing 50 mL of 10% (v/v) HF solution. The tubes were shaken on a shaking bed at 200 rpm for 1 hour at 25 °C, then centrifuged at 3800 rpm for 5 minutes. After discarding the supernatant, the residual soil was subjected to repeated HF treatments under identical conditions. The entire procedure was conducted 8 times with the following shaking durations: 1 hour for the first 4 cycles, 12 hours for cycles 5-7, and 24 hours for the final cycle. The treated residue was washed 5-6 times with distilled water to remove the HF solution. The residue was dried in an oven at 40 °C and sieved through 0.25 mm sieve. Subsequently, pretreated samples were analyzed using a Bruker AVANCE III HD 600MHz spectrometer equipped with an H/X dual-resonance solid probe, operating in CP/MAS mode. Experimental parameters were set as follows: 4-mm ZrO₂ rotor spinning at 10 kHz, ¹³C detection resonance frequency of 150 MHz, acquisition time of 6.25 μs, and spectral width of 30 kHz.

The spectra of samples were divided in the following chemical shift regions: 0–45 ppm (alkyl C, originating from Microbial metabolites and plant biopolymers), 45–110 ppm (O-alkyl C, derived from carbohydrates), 110–160 ppm (aromatic C, derived from lignin, polypeptides and black carbon) and 160–220 ppm (carbonyl C, derived from fatty acids, amino acids and lipids). The relative abundances of different carbon functional groups were quantitatively determined by integrating their respective peak areas in the solid-state ¹³C NMR spectra. Subsequent spectral analyses were performed using MestReNova software (12.0.0-20080) for statistical interpretation of the data. SOC spectra of the different communities are provided in the Appendix A (Fig. S1). According to (Boeni et al., 2014; Wang et al., 2023), four indicators of the stability of SOC were calculated as:

(1) A/O-A, which is used to indicate the degree of humification of SOC, the higher the value, the more resistant it is to decomposition

(2) Alip/Arom, which is used to indicate the complexity of the molecular structure of humus, the higher the ratio, the simpler the molecular structure;

$$\text{Alip/Arom} = (\text{alkyl C} + \text{O-alkyl C}) / \text{aromatic C}$$



226 (3) aromaticity index (AI), which is used as measure of the complexity of SOC
227 structure;

228 $AI = \text{aromatic C} / (\text{alkyl C} + \text{O-alkyl C} + \text{aromatic C})$

229 (4) hydrophobicity index (HI), which is used to indicate the stability of SOC
230 integrated with aggregates.

231 $HI = (\text{alkyl C} + \text{aromatic C}) / (\text{O-alkyl C} + \text{carbonyl C})$

232 **2.6 Statistical analysis**

233 The Shapiro-Wilk test and the Levene test are used respectively to test the
234 regularity and consistency of the data. Differences between community were evaluated
235 through one-way analysis of variance (ANOVA); multiple comparisons were performed
236 using the least significant difference (LSD) test. Nonparametric tests were used for data
237 that did not meet homogeneity of variance. A threshold of $P < 0.05$ was used to denote
238 statistically significant differences. Source contributions were quantified using the
239 “MixSIAR” package in R.

240

241 **3 Results**

242 **3.1 Hydrological Characteristics of East, South and West Dongting Lakes**

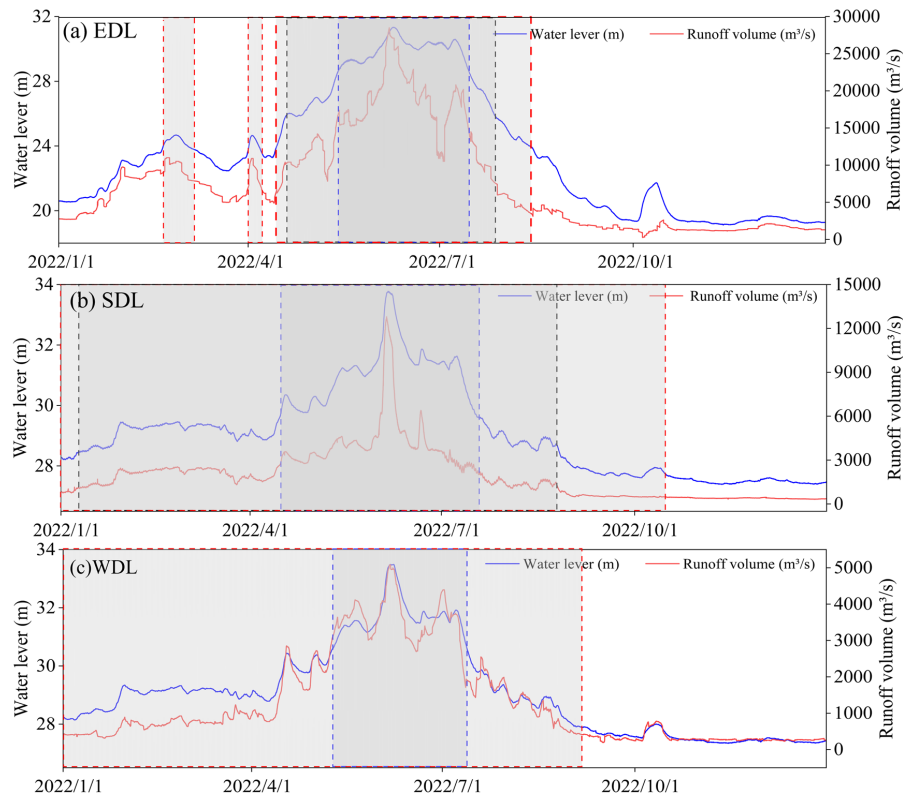


Figure 2. Water level, Runoff volume and inundation duration in EDL, SDL, and WDL. In the figure, the shaded part represents submerged, with the red, black, and blue dashed boxes respectively indicating the Mudflat, *Carex*, and *Miscanthus* communities. EDL: East Dongting Lake; SDL: South Dongting Lake; WDL: West Dongting Lake.

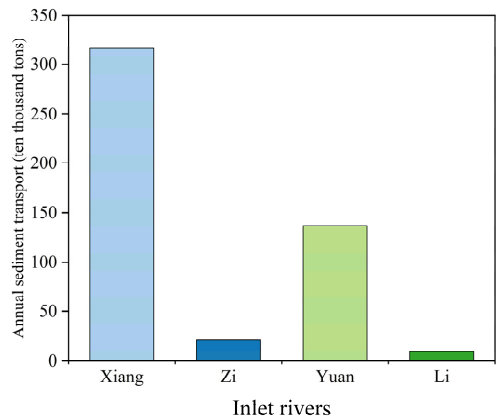


Figure 3. The annual sediment transport of inlet rivers in 2022.



The water level of Dongting Lake shows significant fluctuations (19.24-33.78 m) (Fig.2). There were differences in the inundation duration of different vegetation communities, with the Mudflat having the longest inundation duration (223.8 d), followed by *Carex* (162.4 d), and *Miscanthus* having the shortest inundation time (78.9 d). Among the sub-lakes, SDL showed the longest inundation time (206.8 d), followed by WDL (152 d) and EDL (102.8 d). The annual runoff volume was the highest in EDL, followed by SDL and WDL. The annual sediment transport of four tributaries was 484.1×10^4 tons, with the Xiangjiang River having the highest annual sand transport (Fig.3).

3.2 Carbon sink capacity in dominant vegetation community

The area of Dongting Lake wetland spans 2564.1 km², with vegetation distribution dominated by the *Miscanthus* community (36.9 %), followed by the Mudflat (33.0 %) and the *Carex* community (30.1 %) (Table 1). *Miscanthus* community exhibited significantly higher plant biomass (2922.9 t/km²) and tissue carbon content (454.7 g kg⁻¹) than *Carex* community (1391.0 t/km² and 422.4 g kg⁻¹, respectively; $P < 0.05$). Consequently, its organic carbon stock (1.258 ± 0.13 Tg C) nearly tripled that of *Carex* communities, representing 72.5 % of the wetland's total vegetation-mediated carbon storage.

Table 1

Distribution area, biomass, organic carbon content and carbon stock in dominant vegetation community.

Community types	Areas(km ²)	vegetation biomass (t/km ²)	vegetation organic carbon content (g kg ⁻¹)	vegetation organic carbon storage (Tg C)
<i>Miscanthus</i>	946.74	2922.9±300.8a	454.7±6.22a	1.258±0.13a
<i>Carex</i>	770.63	1391.0±269.7b	422.4±4.75b	0.453±0.09b
<i>Mudflat</i>	846.72	0	0	0

3.3 Stable isotope of soil and vegetation

Miscanthus plants displayed the most enriched $\delta^{13}\text{C}$ values (-13.85 ‰ to -17.24 ‰), contrasting with plankton-derived carbon showing the most depleted signatures. Conversely, $\delta^{15}\text{N}$ values followed an inverse pattern, with plankton exhibiting the highest enrichment (Table 2). There were differences in SOC and TN



276 contents among community types, with the *Miscanthus* and *Carex* communities having
277 significantly higher SOC and TN contents than the Mudflat community ($P < 0.05$, Fig.
278 4a).

279 The soil $\delta^{13}\text{C}$ value ranged from -30.85 to -18.01‰ ($-25.30 \pm 0.54\text{‰}$) with the
280 highest values were observed in *Miscanthus* (-18.01 to -26.08‰) ($P < 0.05$, Fig. 4a),
281 followed by *Mudflat* (-24.3 to -28.68‰) and *Carex* (-27.08 to -30.85‰). There was
282 no significant difference in soils $\delta^{15}\text{N}$ values from different vegetation types. EDL
283 *Carex* communities were smaller in $\delta^{13}\text{C}$ compared to SDL ($P < 0.05$, Fig. 4b), while
284 other vegetation types showed no significant inter-regional differences in SOC, TN,
285 $\delta^{13}\text{C}$ or $\delta^{15}\text{N}$ across sub-basins (Fig. 4b).

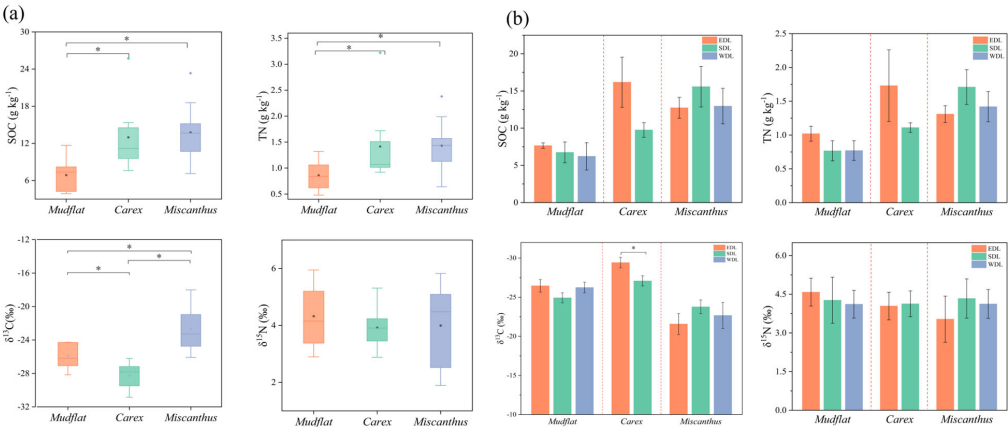
286 **Table 2**

287 Carbon and nitrogen stable isotope signatures (‰) of different potential end-members

Sources	$\delta^{13}\text{C}$ (‰)	$\delta^{15}\text{N}$ (‰)
<i>Miscanthus</i> Plant	-14.46 ± 0.63	0.2 ± 1.45
<i>Carex</i> Plant	-29.51 ± 0.27	2.42 ± 1.03
EDL+SDL POM	-29.31 ± 1.08	6.38 ± 1.5
WDL POM	-29.22 ± 1.40	6.08 ± 1.82
Plankton*	-30.0 ± 6.60	6.5 ± 0.75

294 * C and N stable isotope signature of Plankton were cited from (Kendall et al., 2001;
295 Li et al., 2016)

296



297

298 **Figure 4.** Characteristics of SOC, TN, $\delta^{13}\text{C}$ and $\delta^{15}\text{N}$ with vegetation types (a), and in

299 different sub lakes(b). EDL: East Dongting Lake; SDL: South Dongting Lake; WDL:

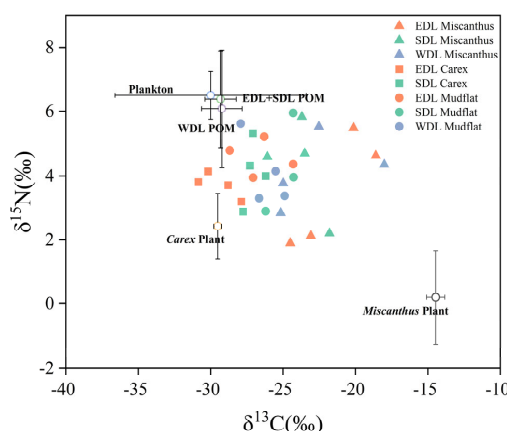


300 West Dongting Lake.

301 3.4 SOC sources and contribution

302 The isotopic composition of all soil samples fell within the mixing space
303 delineated by potential end-members, confirming their effectiveness in source
304 discrimination (Fig. 5). Our study showed autochthonous plant (including *Miscanthus*
305 and *Carex* plant) was the main source of SOC in Dongting floodplain wetland
306 (*Miscanthus*: 53.3 ± 10.6 %, *Carex*: 52.4 ± 11.6 %, Mudflat: 47.5 ± 12.5 %)(Fig. 6a).
307 Allochthonous POM contributions exhibited significant variation across vegetation
308 types, with minimum values in *Miscanthus* communities (26.8 ± 8.1 %) versus *Carex*
309 (31.3 ± 8.3 %) and mudflat (35.4 ± 10.2 %).

310 Spatial heterogeneity in carbon source contributions was evident across vegetation
311 types (Fig. 6b). In *Miscanthus* communities, EDL demonstrated maximal
312 autochthonous input dominance (12.1% and 13.9% greater than SDL and WDL
313 respectively), whereas allochthonous POM displayed inverse spatial patterns (10.9%
314 and 4.7% lower than SDL and WDL respectively). In *Carex* communities, EDL showed
315 8.1% higher in autochthonous contributions relative to SDL, concomitant with 9.1%
316 reduce in POM inputs compared to SDL.



317
318 **Figure 5.** The end-element plots of $\delta^{13}\text{C}$ and $\delta^{15}\text{N}$ values for samples of Dongting Lake
319 soil and SOC sources. EDL: East Dongting Lake; SDL: South Dongting Lake; WDL:
320 West Dongting Lake.

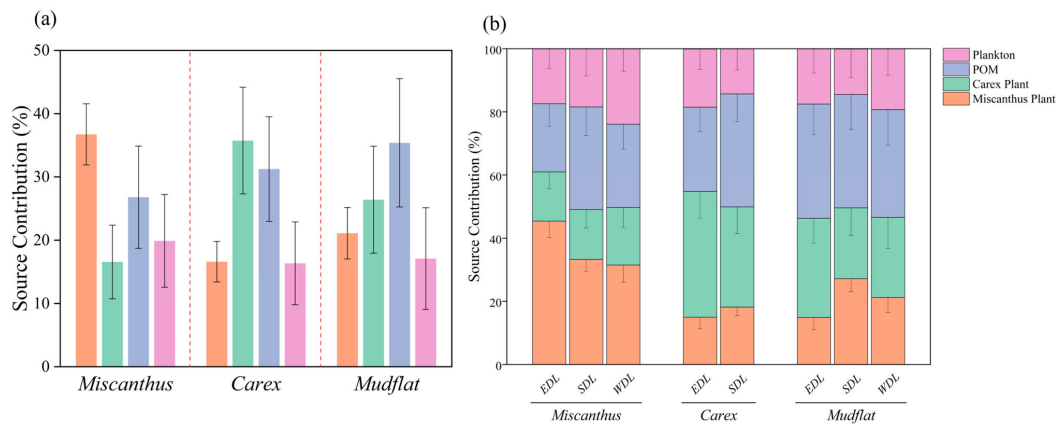


Figure 6. Relative contributions of SOC sources with vegetation types (a) and in different sub lakes (b). POM: particulate organic matter; EDL: East Dongting Lake; SDL: South Dongting Lake; WDL: West Dongting Lake.

3.5 Chemical structure and SOC stability

SOC functional groups were dominated by O-alkyl C (27.3–46.8 %), followed by alkyl C (17.8–41.7 %) and aromatic C (15.5–26.6 %), with Carbonyl C exhibiting minimal abundance. The highest abundance of alkyl C was observed in Mudflat community (25.4 ± 1.2 %), followed by *Carex* (23.2 ± 0.9 %), and then *Miscanthus* community (22.1 ± 0.6 %) ($P < 0.05$, Fig. 7a); O-alkyl C shows the opposite trend. The abundances of aromatic C were significantly higher in the *Carex* community than *Miscanthus* (Fig. 7a, $P < 0.05$). Carbonyl C showed the same trend as alkyl C. There were no significant changes in the abundance of SOC functional groups across vegetation types in different sub lakes (Fig. 7b).

Stability indices showed that Mudflat and *Carex* communities had significantly higher A/O-A ratios, HI indices and aromaticity than *Miscanthus* ($P < 0.05$), while the Alip/Arom ratio showed the opposite pattern (Fig. 8), suggesting that the Mudflat and *Carex* community formed a more stable organic carbon pool through enrichment of difficult-to-degrade fractions, such as alkyl C and aromatic C.

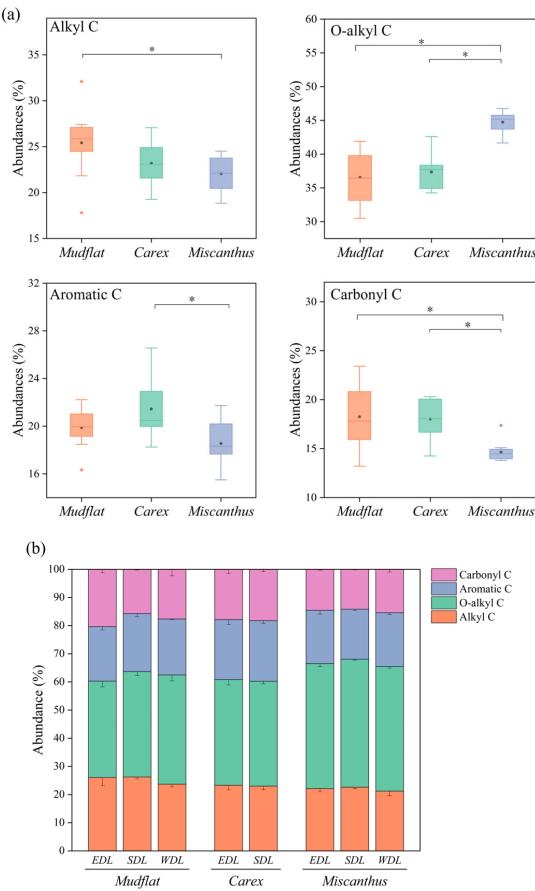


Figure 7. SOC functional group abundance in different vegetation types (a) and in different sub lakes (b). EDL: East Dongting Lake; SDL: South Dongting Lake; WDL: West Dongting Lake.

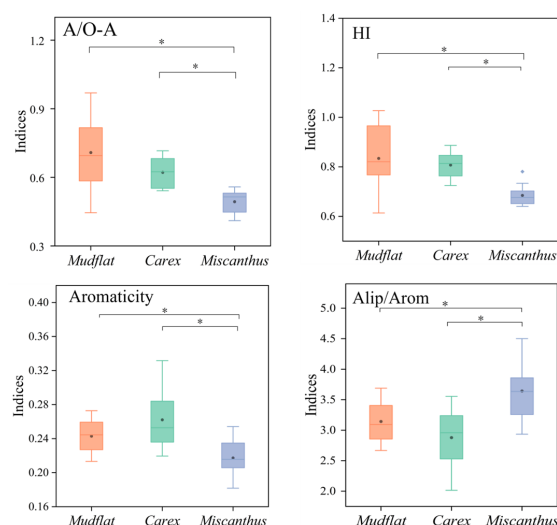


Figure 8. SOC stability index for different vegetation types. A/O-A: the ratio of alkyl C over O-alkyl C; HI: hydrophobicity index, the ratio of the sum of alkyl and aromatic C over the sum of O-alkyl and carbonyl C; Alip/Arom, the ratio of the sum of alkyl C and O-alkyl C over aromatic C; AI, aromaticity index, the ratio of aromatic C over the sum of alkyl C, O-alkyl C and aromatic C.

4 Discussion

4.1 SOC content in different vegetation types

Our study showed that the SOC content of Mudflat community (6.88 g kg^{-1}) was the lowest, and there was no significant difference in SOC content between the two communities (*Miscanthus*: 13.76 g kg^{-1} and *Carex*: 12.99 g kg^{-1}). These results partially support our first hypothesis that SOC content should be the highest in the *Miscanthus* community, followed by the *Carex* community, with the Mudflat exhibiting the lowest SOC content. Although the vegetation biomass of *Miscanthus* community ($2922.9 \pm 300.8 \text{ t/km}^2$) was significantly higher than that of *Carex* community ($1391.0 \pm 269.7 \text{ t/km}^2$), the simpler chemical structure of *Miscanthus* SOC (Fig.7) may facilitate its microbial decomposition. The cross-sub-lake comparisons revealed no significant spatial heterogeneity in vegetated SOC content, which was also inconsistent to our first hypothesis. This may be due to the joint influence of vegetation, hydrology and human



368 disturbance on SOC content.

369 **4.2 SOC sources in different vegetation types**

370 Our results showed that autochthonous plant were the main source of SOC
371 (*Miscanthus*: $53.3 \pm 10.6\%$, *Carex*: $52.4\% \pm 11.6\%$, Mudflat: $47.5 \pm 12.5\%$), which
372 partially supports our second hypothesis that SOC in *Miscanthus* and *Carex* community
373 would primarily originate from autochthonous plant sources; the source of SOC in the
374 Mudflat would primarily originate from allochthonous POM. The SOC of *Miscanthus*
375 and *Carex* communities is mainly derived from autochthonous plant which were related
376 to the plant biomass of communities (*Miscanthus*: 2922.9 ± 300.8 t/km², *Carex*:
377 1391.0 ± 269.7 t/km²) (Table 1). Each year autochthonous plants input a large source of
378 carbon into the soil (Zhu et al., 2022). SOC in the mudflat community was also
379 predominantly derived from autochthonous plants, which can be attributed to reduced
380 allochthonous POM inputs. The commissioning of the Three Gorges Dam in 2003, the
381 world's largest hydropower project, fundamentally altered sediment dynamics, reducing
382 downstream sediment transport from 120×10^6 tons/year (pre-dam) to a state of net
383 erosion (2×10^6 tons/year post-dam) (Yu et al., 2018). The reductions in river sediment
384 transport diminished allochthonous POM contributions. Autochthonous plants are also
385 a major source of SOC in Poyang Lake (located in the lower reaches of the Yangtze
386 River), riverine wetlands along Mexico's Pacific coast, and coastal wetlands in the
387 Mississippi River delta (Wang et al., 2016; Kelsall et al., 2023; Adame and Fry, 2016).
388 The source of SOC in Dongting floodplain wetland has a part of the source of plankton
389 (14.3-23.9 %). This is due to the decline in water quality of the lakes and the gradual
390 increase in algae as a result of problems such as the increased intensity of agricultural
391 farming and the use of chemical fertilizers (Ren et al., 2018).

392 POM had the highest SOC contribution to the Mudflat community ($35.4 \pm$
393 10.2%), followed by *Carex* ($31.3 \pm 8.3\%$), and the lowest was *Miscanthus* ($26.8 \pm$
394 8.1%). This may be related to the different elevations of the vegetation communities
395 (*Miscanthus*: >25 m, *Carex*: $22-25$ m, Mudflat: <22 m), where higher elevations lead
396 to shorter inundation times, thus limiting particulate organic matter (POM) deposition.



397 In this study, we also found that SDL exhibited the highest POM contribution (32.5 %),
398 followed by WDL (26.3 %), with EDL showing minimal inputs (21.6 %) in *Miscanthus*
399 communities. A parallel pattern emerged with *Carex* communities, where SDL's POM
400 contribution exceeded EDL by 9.1%. This may be due to the following: Firstly, the
401 intensive agricultural activities and urbanization in the Xiangjiang River basins that
402 have increased soil erosion, making more POM enter the SDL (Xiao et al., 2023).
403 Second, the northern part of the SDL receives a large amount of sediment under the top-
404 supporting effect of the outflow of WDL (Zhang et al., 2019). Third, the inundation
405 duration is the longest in the SDL, followed by the WDL, and the EDL has the shortest
406 inundation duration. The extension of inundation duration can improve the deposition
407 of allochthonous POM (Shen et al., 2020). Studies have also shown that the mean mass
408 accumulative rate (MAR) of the SDL is the highest, followed by the WDL, and the EDL
409 is the lowest (Ran et al., 2023). Thus, the spatial heterogeneity of allochthonous POM
410 contributions to SOC across sub-lakes revealed synergistic controls by anthropogenic
411 and hydrodynamic drivers.

412 **4.3 SOC stability in in different vegetation types**

413 Our findings demonstrate that O-alkyl C, primarily derived from carbohydrates,
414 constitutes the dominant fraction (27.3 – 46.8 %) of SOC in Dongting Lake wetlands.
415 This result partially supports our third hypothesis that the structure of SOC in
416 *Miscanthus* and *Carex* should be dominated by O-alkyl C, and the SOC structure of the
417 Mudflat should be dominated by aromatic C. The predominance of O-alkyl C across
418 vegetation communities likely reflects the autochthonous origin of SOC from plant-
419 derived inputs. Specifically, the cellulose and hemicellulose components of plant litter
420 decompose rapidly to produce carbohydrates (Mckee et al., 2016), which is consistent
421 with findings from other lake or river wetlands where O-alkyl C represents the principal
422 SOC fraction (Yang et al., 2023; Wang et al., 2011)

423 Notably, the *Miscanthus* community exhibited significantly higher O-alkyl C
424 content compared to *Carex* and mudflat, while displaying lower alkyl and aromatic C
425 contents (Fig. 7a). Given that O-alkyl C was classified as labile C whereas alkyl and



426 aromatic C were classified as recalcitrant C, these results showed that *Miscanthus*
427 community SOC is more unstable and more susceptible to decomposition. Therefore,
428 the risk of SOC loss is higher in the *Miscanthus* community. The A/O-A and aromaticity
429 as well as HI and Alip/Arom, are recognized as important parameters for evaluating the
430 stability of SOC. The A/O-A ratio, aromaticity and hydrophobicity index (HI) were
431 significantly higher in the *Carex* and mudflat communities than *Miscanthus* community
432 ($P < 0.05$), whereas the Alip/Arom ratio showed the opposite trend, indicating that the
433 SOC of *Carex* and mudflat communities had more complex structures and higher
434 hydrophobicity, which increased SOC stability (Spaccini et al., 2006).

435 O-alkyl C is primarily derived from carbohydrates. *Miscanthus* plants possess a
436 well-developed underground root system that may produce more root secretions,
437 which are mainly composed of carbohydrates (Wu et al., 2021b). The higher aromatic
438 and alkyl C fractions observed in *Carex* and mudflat communities likely result from
439 prolonged inundation duration, which extends exposure to anaerobic conditions.
440 Anoxic conditions significantly limit reactive oxygen species generation and catalase
441 activity, thereby inhibiting oxidative decomposition of lignin (the main component of
442 aromatic carbon) (Benner et al., 1984; Kirk and Farrell, 1987). Additionally, microbial
443 metabolic efficiency declines under oxygen deprivation, retarding the decomposition of
444 lipids and waxes (alkyl carbon precursors) (Keiluweit et al., 2017). These stability
445 difference may be related to the contribution of allochthonous POM. Allochthonous
446 carbon is rich in aromatic and hydrophobic components, exhibiting stronger resistance
447 to decomposition (Keil, 2011). The proportion of allochthonous POM was significantly
448 higher in the *Carex* and mudflat communities than in the *Miscanthus*.

449 The risk of loss of soil carbon pools in *Miscanthus* community is higher due to
450 the more labile molecular structure of SOC (Fig. 9). In our previous research, we also
451 found that the *Miscanthus* community experienced the greatest loss of SOC from 2013
452 to 2022 (Wang et al., 2025). Although the SOC stability of the *Miscanthus* community
453 is relatively low, its SOC content shows no significant difference from that of the *Carex*
454 community due to high litter input (1.258 ± 0.13 Tg C), revealing the differences in the



mechanisms of carbon sequestration function formation among different vegetation
types in floodplain wetlands (Fig. 9).

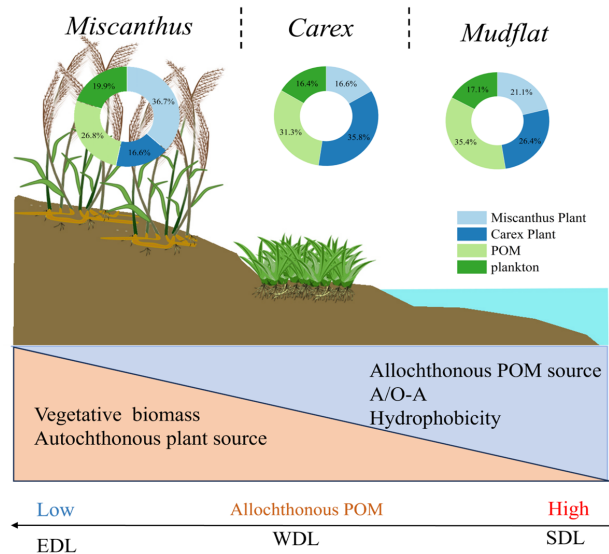


Figure 9. A conceptual map of the sources and stability of SOC on a geomorphic gradient in the Dongting floodplain wetlands. Orange triangles show the decrease in vegetative biomass and autochthonous plant sources from *Miscanthus* (high elevation) to Mudflat (low elevation). In contrast, blue triangles show increases in allochthonous POM sources, A/O-A, and hydrophobicity. The arrows below indicate that from SDL to WDL to EDL, the contribution of allochthonous POM is decreasing. A/O-A: the ratio of alkyl C over O-alkyl C; POM: particulate organic matter; EDL: East Dongting Lake; SDL: South Dongting Lake; WDL: West Dongting Lake.

5 Conclusions

Stable isotopic analysis demonstrates that SOC in Dongting floodplain wetlands was mainly derived from autochthonous plant inputs, with mean contributions of $53.3 \pm 10.6\%$ (*Miscanthus*), $52.4 \pm 11.6\%$ (*Carex*), and $47.5 \pm 12.5\%$ (mudflat). Notably, allochthonous POM contributions exhibited both vegetation-dependent (mudflat > *Carex* > *Miscanthus*) and regional disparities (SDL>WDL>EDL). We attribute these



474 differences to interacting effects of anthropogenic and hydrodynamic drivers, which
475 collectively regulate allochthonous POM transport and deposition. The A/O-A ratios,
476 aromaticity, and hydrophobicity were lower in *Miscanthus* community, indicating that
477 SOC is more easily decomposed, and the stability of SOC pools is lower. Therefore, we
478 should prioritize the conservation of *Miscanthus* communities SOC to mitigate carbon
479 loss risks.

480

481 **Acknowledgments**

482 This work was supported by the National Natural Science Foundation of China
483 (U2444221, U22A20570, U21A2009) and the Natural Science Foundation of Hunan
484 Province(2025JJ20039).

485

486 **Author contributions**

487 LW: Writing – original draft, Investigation, Data curation. ZD: Writing – review &
488 editing, Project administration, Funding acquisition, Conceptualization. YX: Writing–
489 review & editing, Funding acquisition. TW: Investigation, Data curation. FL: Writing–
490 review & editing, Methodology. YZ: Investigation, Data curation. BW: Formal analysis,
491 Resources. ZH: Methodology, Data curation. CZ: Investigation, Data curation. CP:
492 Writing – review & editing, Formal analysis. AM: Formal analysis, Conceptualization.

493

494 **Data availability**

495 Data will be made available upon request.

496

497 **Declaration of Competing Interest**

498 The authors declare that they have no known competing financial interests or personal
499 relationships that could have appeared to influence the work reported in this paper.

500



Reference

- Adame, M. F. and Fry, B.: Source and stability of soil carbon in mangrove and freshwater wetlands of the Mexican Pacific coast, *Wetlands Ecol. Manage.*, 24, 129-137, <http://doi.org/10.1007/s11273-015-9475-6>, 2016.
- Benner, R., Maccubbin, A. E., and Hodson, R. E.: Anaerobic Biodegradation of the Lignin and Polysaccharide Components of Lignocellulose and Synthetic Lignin by Sediment Microflora, *Appl. Environ. Microbiol.*, 47, 998-1004, <http://doi.org/doi:10.1128/aem.47.5.998-1004.1984>, 1984.
- Boeni, M., Bayer, C., Dieckow, J., Conceição, P. C., Dick, D. P., Knicker, H., Salton, J. C., and Macedo, M. C. M.: Organic matter composition in density fractions of Cerrado Ferralsols as revealed by CPMAS ¹³C NMR: Influence of pastureland, cropland and integrated crop-livestock, *Agric., Ecosyst. Environ.*, 190, 80-86, <http://doi.org/10.1016/j.agee.2013.09.024>, 2014.
- Boye, K., Noël, V., Tfaily, M. M., Bone, S. E., Williams, K. H., Bargar, J. R., and Fendorf, S.: Thermodynamically controlled preservation of organic carbon in floodplains, *Nat. Geosci.*, 10, 415-419, <http://doi.org/10.1038/ngeo2940>, 2017.
- Cano, A. F., Mermut, A. R., Ortiz, R., Benke, M. B., and Chatson, B.: ¹³C CP/MAS-NMR spectra, of organic matter as influenced by vegetation, climate, and soil characteristics in soils from Murcia, Spain, *Can. J. Soil Sci.*, 82, 403-411, 2002.
- Chen, X., Xu, Y. J., Gao, H. J., Mao, J. D., Chu, W. Y., and Thompson, M. L.: Biochemical stabilization of soil organic matter in straw-amended, anaerobic and aerobic soils, *Sci. Total Environ.*, 625, 1065-1073, <http://doi.org/10.1016/j.scitotenv.2017.12.293>, 2018.
- Deng, Z. M., Li, Y. Z., Xie, Y. H., Peng, C. H., Chen, X. S., Li, F., Ren, Y. J., Pan, B. H., and Zhang, C. Y.: Hydrologic and Edaphic Controls on Soil Carbon Emission in Dongting Lake Floodplain, China, *Journal of Geophysical Research-Biogeosciences*, 123, 3088-3097, <http://doi.org/10.1029/2018jg004515>, 2018.
- Doetterl, S., Berhe, A. A., Nadeu, E., Wang, Z. G., Sommer, M., and Fiener, P.: Erosion, deposition and soil carbon: A review of process-level controls, experimental tools and models to address C cycling in dynamic landscapes, *Earth-Sci. Rev.*, 154, 102-122, <http://doi.org/10.1016/j.earscirev.2015.12.005>, 2016.
- Jun-feng, G., Chen, Z., Jia-hu, J., and Qun, H.: Analysis of deposition and erosion of Dongting Lake by GIS, *Journal of Geographical Sciences*, 11, 402-410, 2001.
- Kayranli, B., Scholz, M., Mustafa, A., and Hedmark, Å.: Carbon Storage and Fluxes within Freshwater Wetlands: a Critical Review, *Wetlands*, 30, 111-124, <http://doi.org/10.1007/s13157-009-0003-4>, 2010.
- Keil, R. G.: Terrestrial influences on carbon burial at sea, *Proc. Natl. Acad. Sci. U. S. A.*, 108, 9729-9730, <http://doi.org/10.1073/pnas.1106928108>, 2011.
- Keiluweit, M., Wanzek, T., Kleber, M., Nico, P., and Fendorf, S.: Anaerobic microsites have an unaccounted role in soil carbon stabilization, *Nat. Commun.*, 8, <http://doi.org/10.1038/s41467-017-01406-6>, 2017.
- Kelsall, M., Quirk, T., Wilson, C., and Snedden, G. A.: Sources and chemical stability of soil organic carbon in natural and created coastal marshes of Louisiana, *Sci. Total Environ.*, 867, 12, <http://doi.org/10.1016/j.scitotenv.2023.161415>, 2023.
- Kendall, C., Silva, S. R., and Kelly, V. J.: Carbon and nitrogen isotopic compositions of particulate organic matter in four large river systems across the United States, *Hydrol. Processes*, 15, 1301-1346, <http://doi.org/10.1002/hyp.216>, 2001.



- 545 Kirk, T. K. and Farrell, R. L.: ENZYMATIC COMBUSTION - THE MICROBIAL-DEGRADATION
546 OF LIGNIN, *Annu. Rev. Microbiol.*, 41, 465-505,
547 <http://doi.org/10.1146/annurev.mi.41.100187.002341>, 1987.
- 548 Köchy, M., Hiederer, R., and Freibauer, A.: Global distribution of soil organic carbon – Part 1: Masses
549 and frequency distributions of SOC stocks for the tropics, permafrost regions, wetlands, and the
550 world, *SOIL*, 1, 351-365, <http://doi.org/10.5194/soil-1-351-2015>, 2015.
- 551 Li, Y., Zhang, H. B., Tu, C., Fu, C. C., Xue, Y., and Luo, Y. M.: Sources and fate of organic carbon and
552 nitrogen from land to ocean: Identified by coupling stable isotopes with C/N ratio, *Estuar. Coast.*
553 *Shelf Sci.*, 181, 114-122, <http://doi.org/10.1016/j.ecss.2016.08.024>, 2016.
- 554 Liu, S. Y., Li, J. Y., Liang, A. Z., Duan, Y., Chen, H. B., Yu, Z. Y., Fan, R. Q., Liu, H. Y., and Pan, H.:
555 Chemical Composition of Plant Residues Regulates Soil Organic Carbon Turnover in Typical Soils
556 with Contrasting Textures in Northeast China Plain, *Agronomy-Basel*, 12,
557 <http://doi.org/10.3390/agronomy12030747>, 2022.
- 558 McKee, G. A., Soong, J. L., Caldéron, F., Borch, T., and Cotrufo, M. F.: An integrated spectroscopic and
559 wet chemical approach to investigate grass litter decomposition chemistry, *Biogeochemistry*, 128,
560 107-123, <http://doi.org/10.1007/s10533-016-0197-5>, 2016.
- 561 Mitsch, W. J., Bernal, B., Nahlik, A. M., Mander, Ü., Zhang, L., Anderson, C. J., Jorgensen, S. E., and
562 Brix, H.: Wetlands, carbon, and climate change, *Landsc. Ecol.*, 28, 583-597,
563 <http://doi.org/10.1007/s10980-012-9758-8>, 2013.
- 564 Preston, C. M., Newman, R. H., and Rother, P.: USING C-13 CPMAS NMR TO ASSESS EFFECTS OF
565 CULTIVATION ON THE ORGANIC-MATTER OF PARTICLE-SIZE FRACTIONS IN A
566 GRASSLAND SOIL, *Soil Sci.*, 157, 26-35, <http://doi.org/10.1097/00010694-199401000-00005>,
567 1994.
- 568 Quideau, S. A., Chadwick, O. A., Benesi, A., Graham, R. C., and Anderson, M. A.: A direct link between
569 forest vegetation type and soil organic matter composition, *Geoderma*, 104, 41-60,
570 [http://doi.org/10.1016/s0016-7061\(01\)00055-6](http://doi.org/10.1016/s0016-7061(01)00055-6), 2001.
- 571 Ran, F., Nie, X., Wang, S., Liao, W., and Li, Z.: Evolutionary patterns of the sedimentary environment
572 signified by grain size characteristics in Lake Dongting during the last century, *Journal of Lake*
573 *Sciences*, 35, 1111-1125, 2023.
- 574 Ren, J. L., Zheng, Z. B., Li, Y. M., Lv, G. N., Wang, Q., Lyu, H., Huang, C. C., Liu, G., Du, C. G., Mu,
575 M., Lei, S. H., and Bi, S.: Remote observation of water clarity patterns in Three Gorges Reservoir
576 and Dongting Lake of China and their probable linkage to the Three Gorges Dam based on Landsat
577 8 imagery, *Sci. Total Environ.*, 625, 1554-1566, <http://doi.org/10.1016/j.scitotenv.2018.01.036>,
578 2018.
- 579 Robertson, A. I., Bunn, S. E., Boon, P. I., and Walker, K. F.: Sources, sinks and transformations of organic
580 carbon in Australian floodplain rivers, *Mar. Freshw. Res.*, 50, 813-829,
581 <http://doi.org/10.1071/mf99112>, 1999.
- 582 Sasmito, S. D., Kuzyakov, Y., Lubis, A. A., Murdiyarso, D., Hutley, L. B., Bachri, S., Friess, D. A.,
583 Martius, C., and Borchard, N.: Organic carbon burial and sources in soils of coastal mudflat and
584 mangrove ecosystems, *Catena*, 187, 11, <http://doi.org/10.1016/j.catena.2019.104414>, 2020.
- 585 Shen, D. Y., Ye, C. L., Hu, Z. K., Chen, X. Y., Guo, H., Li, J. Y., Du, G. Z., Adl, S., and Liu, M. Q.:
586 Increased chemical stability but decreased physical protection of soil organic carbon in response to
587 nutrient amendment in a Tibetan alpine meadow, *Soil Biol. Biochem.*, 126, 11-21,
588 <http://doi.org/10.1016/j.soilbio.2018.08.008>, 2018.



- 589 Shen, R. C., Lan, Z. C., Huang, X. Y., Chen, Y. S., Hu, Q. W., Fang, C. M., Jin, B. S., and Chen, J. K.:
590 Soil and plant characteristics during two hydrologically contrasting years at the lakeshore wetland
591 of Poyang Lake, China, *J. Soils Sediments*, 20, 3368-3379, [http://doi.org/10.1007/s11368-020-](http://doi.org/10.1007/s11368-020-02638-8)
592 [02638-8](http://doi.org/10.1007/s11368-020-02638-8), 2020.
- 593 Skjemstad, J. O., Clarke, P., Taylor, J. A., Oades, J. M., and Newman, R. H.: THE REMOVAL OF
594 MAGNETIC-MATERIALS FROM SURFACE SOILS - A SOLID-STATE C-13 CP/MAS NMR-
595 STUDY, *Aust. J. Soil Res.*, 32, 1215-1229, <http://doi.org/10.1071/sr9941215>, 1994.
- 596 Spaccini, R., Mbagwu, J. S. C., Conte, P., and Piccolo, A.: Changes of humic substances characteristics
597 from forested to cultivated soils in Ethiopia, *Geoderma*, 132, 9-19,
598 <http://doi.org/10.1016/j.geoderma.2005.04.015>, 2006.
- 599 Wang, F. F., Tao, Y. R., Yang, S. C., and Cao, W. Z.: Warming and flooding have different effects on
600 organic carbon stability in mangrove soils, *J. Soils Sediments*, 10, [http://doi.org/10.1007/s11368-](http://doi.org/10.1007/s11368-023-03636-2)
601 [023-03636-2](http://doi.org/10.1007/s11368-023-03636-2), 2023.
- 602 Wang, F. F., Zhang, N., Yang, S. C., Li, Y. S., Yang, L., and Cao, W. Z.: Source and stability of soil organic
603 carbon jointly regulate soil carbon pool, but source alteration is more effective in mangrove
604 ecosystem following *Spartina alterniflora* invasion, *Catena*, 235, 12,
605 <http://doi.org/10.1016/j.catena.2023.107681>, 2024a.
- 606 Wang, J. J., Dodla, S. K., DeLaune, R. D., Hudnall, W. H., and Cook, R. L.: Soil Carbon Characteristics
607 in Two Mississippi River Deltaic Marshland Profiles, *Wetlands*, 31, 157-166,
608 <http://doi.org/10.1007/s13157-010-0130-y>, 2011.
- 609 Wang, L., Wang, B., Deng, Z., Xie, Y., Wang, T., Li, F., Wu, S. a., Hu, C., Li, X., and Hou, Z.: Surface
610 soil organic carbon losses in Dongting Lake floodplain as evidenced by field observations from
611 2013 to 2022, *J. Integr. Agric.*, 2025.
- 612 Wang, M., Lai, J., Hu, K., and Zhang, D.: Compositions of stable organic carbon and nitrogen isotopes
613 in wetland soil of Poyang Lake and its environmental implications, *China Environmental Science*,
614 36, 500-505, 2016.
- 615 Wang, S. L., Ran, F. W., Li, Z. W., Yang, C. R., Xiao, T., Liu, Y. J., and Nie, X. D.: Coupled effects of
616 human activities and river-Lake interactions evolution alter sources and fate of sedimentary organic
617 carbon in a typical river-Lake system, *Water Res.*, 255, 13,
618 <http://doi.org/10.1016/j.watres.2024.121509>, 2024b.
- 619 Wu, H., Zhang, H. C., Chang, F. Q., Duan, L. Z., Zhang, X. N., Peng, W., Liu, Q., Zhang, Y., and Liu, F.
620 W.: Isotopic constraints on sources of organic matter and environmental change in Lake Yangzong,
621 Southwest China, *Journal of Asian Earth Sciences*, 217, 11,
622 <http://doi.org/10.1016/j.jseaes.2021.104845>, 2021a.
- 623 Wu, J. P., Deng, Q., Hui, D. F., Xiong, X., Zhang, H. L., Zhao, M. D., Wang, X., Hu, M. H., Su, Y. X.,
624 Zhang, H. O., Chu, G. W., and Zhang, D. Q.: Reduced Lignin Decomposition and Enhanced Soil
625 Organic Carbon Stability by Acid Rain: Evidence from ¹³C Isotope and ¹³C NMR Analyses, *Forests*,
626 11, 14, <http://doi.org/10.3390/f11111191>, 2020.
- 627 Wu, Q., Lin, Y., Sun, Y., Wei, Q., Liu, J., Li, X., and Cui, G.: Research Progress on Effects of Root
628 Exudates on Plant Growth and Soil Nutrient Uptake, *Chinese Journal of Grassland*, 43, 97-104,
629 2021b.
- 630 Xiao, T., Ran, F. W., Li, Z. W., Wang, S. L., Nie, X. D., Liu, Y. J., Yang, C. R., Tan, M., and Feng, S. R.:
631 Sediment organic carbon dynamics response to land use change in diverse watershed anthropogenic
632 activities, *Environ. Int.*, 172, <http://doi.org/10.1016/j.envint.2023.107788>, 2023.



- 633 Xie, Y. H., Yue, T., Chen, X. S., Feng, L., and Deng, Z. M.: The impact of Three Gorges Dam on the
634 downstream eco-hydrological environment and vegetation distribution of East Dongting Lake,
635 *Ecohydrology*, 8, 738-746, <http://doi.org/10.1002/eco.1543>, 2015.
- 636 Yang, Y., Jia, G. D., Yu, X. X., and Cao, Y. X.: Land use conversion impacts on the stability of soil organic
637 carbon in Qinghai Lake using ^{13}C NMR and C cycle-related enzyme activities, *Land Degrad. Dev.*,
638 34, 3606-3617, <http://doi.org/10.1002/ldr.4706>, 2023.
- 639 Yu, Y. W., Mei, X. F., Dai, Z. J., Gao, J. J., Li, J. B., Wang, J., and Lou, Y. Y.: Hydromorphological
640 processes of Dongting Lake in China between 1951 and 2014, *J. Hydrol.*, 562, 254-266,
641 <http://doi.org/10.1016/j.jhydrol.2018.05.015>, 2018.
- 642 Zhang, J. Q., Hao, Q., Li, Q., Zhao, X. W., Fu, X. L., Wang, W. Q., He, D., Li, Y., Zhang, Z. Q., Zhang,
643 X. D., and Song, Z. L.: Source identification of sedimentary organic carbon in coastal wetlands of
644 the western Bohai Sea, *Sci. Total Environ.*, 913, <http://doi.org/10.1016/j.scitotenv.2023.169282>,
645 2024.
- 646 Zhang, W. L., Gu, J. F., Li, Y., Lin, L., Wang, P. F., Wang, C., Qian, B., Wang, H. L., Niu, L. H., Wang,
647 L. F., Zhang, H. J., Gao, Y., Zhu, M. J., and Fang, S. Q.: New Insights into Sediment Transport in
648 Interconnected River-Lake Systems Through Tracing Microorganisms, *Environ. Sci. Technol.*, 53,
649 4099-4108, <http://doi.org/10.1021/acs.est.8b07334>, 2019.
- 650 Zhu, L. L., Deng, Z. M., Xie, Y. H., Zhang, C. Y., Chen, X. R., Li, X., Li, F., Chen, X. S., Zou, Y. A., and
651 Wang, W.: Effects of hydrological environment on litter carbon input into the surface soil organic
652 carbon pool in the Dongting Lake floodplain, *Catena*, 208,
653 <http://doi.org/10.1016/j.catena.2021.105761>, 2022.
- 654